

# Hyperbranched Polymers: Structure of Hyperbranched Polyglycerol and Amphiphilic Poly(glycerol ester)s in Dilute Aqueous and Nonaqueous Solution

Vasil M. Garamus,<sup>†</sup> Tatiana V. Maksimova,<sup>‡</sup> Holger Kautz,<sup>§</sup> Emilie Barriau,<sup>§</sup> Holger Frey,<sup>§</sup> Ulf Schlotterbeck,<sup>⊥</sup> Stefan Mecking<sup>⊥</sup> and Walter Richtering<sup>\*,‡</sup>

GKSS Research Centre, Max Planck Str., D-21502 Geesthacht, Germany; Physical Chemistry II, RWTH Aachen University, Templergraben 59, D-52056 Aachen, Germany; Institute of Organic Chemistry, Organic and Macromolecular Chemistry, Johannes-Gutenberg-University Mainz, Duesbergweg 10-14, D-55128 Mainz, Germany; and Chemistry Department, Konstanz University, Universitätsstr. 10, D-78457 Konstanz, Germany

**ABSTRACT:** The solution structure of hyperbranched macromolecules was investigated by means of small-angle neutron scattering (SANS). Hyperbranched polyglycerols of different molecular weight were investigated in D<sub>2</sub>O and CD<sub>3</sub>OD, and very similar molar masses and radii of gyration were obtained in both solvents. Kratky plots of the scattering intensity revealed a compact structure of the hyperbranched polyglycerols. A power law scaling relation of the radius of gyration with molar mass was observed, from which a dimension of three was obtained. These observations indicate that the hyperbranched structure prevents strong irregular association despite the high functionality of hydroxyl groups that could lead to aggregation in those solvents. Amphiphilic derivatives of the hyperbranched polyglycerols have been studied in the nonpolar solvent C<sub>6</sub>D<sub>6</sub>. Again, molecularly dispersed polymers were found provided the degree of esterification was sufficiently high. A low degree of derivatization of only 22% was not sufficient to prevent aggregation in C<sub>6</sub>D<sub>6</sub>. The macromolecules become more compact when the degree of esterification increases.

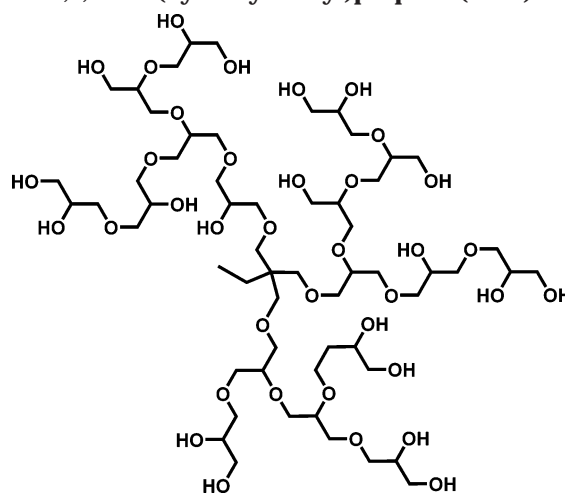
## Introduction

Hyperbranched polymers are macromolecules with random branch-on-branch topology and compact molecular dimensions. Topologically, they contain no connection line between any two end groups that passes all branching points. In nature this structural principle is ubiquitously present e.g. in polysaccharides such as glycogen, dextran, and amylopectin. The general understanding of their structural composition dates back to the 1930s.<sup>1</sup>

In 1952, Flory introduced the concept for their man-made synthesis based on step by step-growth polymerization of multifunctional AB<sub>n</sub> monomers.<sup>2</sup> But only within the past 10 years, synthetic hyperbranched macromolecules found a rapidly growing interdisciplinary interest highly profiting from the fascination created by the structurally perfect dendrimers.

Most applications of multiply branched polymers are based on the absence of chain entanglements and the nature and the large number of functional groups within a molecule. The functionality of hyperbranched polymers allows for the tailoring of their chemical, thermal, rheological, and solution properties and thus provides a powerful tool to design polymers for a wide variety of applications.<sup>3–6</sup> Unlike dendrimers, hyperbranched polymers with similar properties can be easily synthesized via one-step reactions<sup>7</sup> and therefore represent economically promising products for large-scale industrial applications. Their molecular architecture is usually not

**Scheme 1. Schematic Drawing of Hyperbranched Poly(glycerol) Initiated by 1,1,1-Tris(hydroxymethyl)propane (TMP)**



as well-defined as for dendrimers, and their molecular mass distribution is not monodisperse. However, a recent development<sup>8,9</sup> paved the way for unprecedentedly well-defined hyperbranched polyether polyols,<sup>10</sup> which are the starting point of our scattering studies. The general structure of hyperbranched polyglycerol is displayed in Scheme 1.

Because of the limited number of hyperbranched model systems with controlled molar mass and low polydispersities, scattering studies addressing them are still scarce. Gelade et al.<sup>11</sup> and de Luca et al.<sup>12</sup> reported SANS experiments on fractionated hyperbranched poly-(ester amide)s and polyesters in organic solvents. They

<sup>†</sup> GKSS Research Centre.

<sup>‡</sup> RWTH Aachen University.

<sup>§</sup> Johannes-Gutenberg-University Mainz.

<sup>⊥</sup> Konstanz University.

\* Corresponding author. E-mail: richtering@rwth-aachen.de.

obtained the molecular weight,  $M_w$ , and discussed the radius of gyration,  $R_g$ , the second virial coefficient,  $A_2$ , and the zero shear viscosity,  $\eta_0$ , as a function of  $M_w$ . The fractal dimension,  $d_f$ , was obtained from the power-law decay of the form factor at intermediate values of scattering vector  $q$  and from the scaling behavior of  $R_g$  and  $\eta_0$  with molecular weight. The fractal dimensions range from 2 to 2.5.

In recent work, some of us demonstrated that hyperbranched polyglycerols with amphiphilic core-shell structure ("molecular nanocapsules"), conveniently prepared in two synthetic steps, exhibit unimolecular reverse micelle properties, i.e., encapsulation and phase transfer of ionic guest molecules in analogy to amphiphilic dendrimers.<sup>13,14</sup> A partial esterification of hyperbranched polyglycerols using fatty acid chlorides provided the amphiphilic polyglycerols that quantitatively extract various dyes from the aqueous phase into apolar media, stabilize nanosize palladium colloids,<sup>15-18</sup> and are able to extract catalytically active polar pincer Pt(II) complexes.<sup>19,20</sup> The intriguing phase transfer properties of hyperbranched polyglycerol nanocapsules have been explained by their hydrophobic shell/hydrophilic core structure. However, there is still very little detailed information on the solution structure of such polyglycerol derivatives.

In this contribution we report on dilute solution properties of water-soluble, hyperbranched polyglycerols. The solutions were investigated by means of small-angle neutron scattering in two solvents, namely  $D_2O$  and deuterated methanol ( $CD_3OD$ ). In addition, we studied amphiphilic derivatives of hyperbranched polyglycerol. Dilute solutions of poly(glycerol ester)s with different degrees of esterification were investigated by SANS in deuterated benzene ( $C_6D_6$ ) as apolar organic solvent.

## Experimental Section

The synthesis of the polyglycerols and their derivatization with palmitoyl chloride was performed as described previously.<sup>10</sup> Small-angle neutron scattering experiments have been carried out at the SANS1 instrument at the FRG1 research reactor at GKSS Research Centre, Geestacht, Germany.<sup>21</sup> The measurements have been performed with a neutron wavelength of  $\lambda = 0.81$  nm and a wavelength resolution of  $(\Delta\lambda/\lambda) = 10\%$ . A range of scattering vectors of  $0.05 < q < 2.5$  nm<sup>-1</sup> was obtained. As deuterated solvents, heavy water ( $D_2O$ ) and methanol- $d_4$  ( $CD_3OD$ ) for polyglycerol and  $C_6D_6$  for poly(glycerol ester)s were used. Dilute polyglycerol solutions were measured at 25 °C in Hellma quartz cells with a path length of 2 mm. The raw spectra were corrected for backgrounds from the solvent, sample cell, and other sources by conventional procedures. The two-dimensional isotropic scattering spectra were azimuthally averaged, converted to an absolute scale, and corrected for detector efficiency by dividing by the incoherent scattering spectrum of pure water in a 1 mm quartz cell.

Partial volumes of some polymers were determined with a Paar densitometer. For polyglycerol the partial volume is 0.75 cm<sup>3</sup>g<sup>-1</sup> in  $D_2O$  and 0.82 cm<sup>3</sup>g<sup>-1</sup> in  $CD_3OD$ . The partial volume of the poly(glycerol ester)s in  $C_6D_6$  was determined for a series of samples with different degrees of esterification: PG6000-C15<sub>0.22</sub>, 0.95 cm<sup>3</sup>g<sup>-1</sup>; PG6000-C15<sub>0.48</sub>, 1.01 cm<sup>3</sup>g<sup>-1</sup>; PG6000-C15<sub>0.77</sub>, 1.04 cm<sup>3</sup>g<sup>-1</sup>; PG6000-C15<sub>1.00</sub>, 1.06 cm<sup>3</sup>g<sup>-1</sup>.

## Results and Discussion

Small-angle neutron scattering provides information on shape, size, and interactions of the scattering entities over a broad range of length scales ranging from nanometers up to microns. The intensity  $I(q)$  of the

scattered neutrons is measured as a function of the magnitude of the scattering vector  $q = (4\pi/\lambda) \sin(\theta/2)$ . Here,  $\lambda$  denotes the neutron wavelength and  $\theta$  is the scattering angle. Similar to light scattering, the scattering intensity in dilute solution, when interactions can be neglected, is given as<sup>22</sup>

$$I(q) = cK_{\text{SANS}}M_wP(q) \quad (1)$$

where  $c$  is the concentration in mass per volume,  $M_w$  the weight-average molar mass, and  $K_{\text{SANS}}$  a contrast factor given as

$$K_{\text{SANS}} = \bar{v}^2(\Delta\rho)^2/N_L \quad (2)$$

with  $\bar{v}$  partial volume of the polymer,  $\Delta\rho$  the excess scattering length density, and  $N_L$  Avogadro's constant.

Nonnegligible polymer interactions at finite concentration influence the scattering intensity, and an apparent molecular weight  $M_{\text{app}}$  is obtained at zero scattering angle. The concentration dependence in the dilute regime is described by a virial expansion with the second virial coefficient  $A_2$ .

$$\frac{K_{\text{SANS}}c}{I(q=0)} = \frac{1}{M_{\text{app}}(c)} = \frac{1}{M_w} + 2A_2c + \dots \quad (3)$$

The form factor  $P(q)$  yields information about the structure of a single particle (intraparticle) correlations and has been calculated for various polymer architectures. In the limit of small scattering vectors the  $z$ -average radius of gyration  $R_g = \langle S^2 \rangle_z^{0.5}$  is obtained from the initial slope. The extrapolation to zero scattering angle for the determination of  $I(0)$  and the  $z$ -averaged radius of gyration  $R_g$  was performed within the Guinier approximation:

$$I(q) = I(0) \exp\left(-\frac{1}{3}q^2\langle S^2 \rangle_z\right) \quad (4)$$

Neglecting excluded-volume effects, which means assuming Gaussian statistics, Burchard<sup>23</sup> determined the form factor of a nonrandom  $AB_f$  polycondensate to be

$$P(q) = \left(1 + \frac{1}{6}q^2\langle S^2 \rangle_z\right)^{-2} \quad (5)$$

The form factor given in eq 5 exhibits a pronounced maximum in a Kratky representation, where  $q^2I(q)$  is plotted vs  $q$ . From the peak location at  $q = q_{\text{max}}$  the radius of gyration can be obtained.

$$q_{\text{max}}R_g = \sqrt{6} \quad (6)$$

**Hyperbranched Polyglycerols.** Figure 1 (top and bottom) shows the  $q$  dependence of the measured neutron scattering intensity of polyglycerol (PG) solution normalized by the polymer concentration in  $D_2O$  (top) and  $CD_3OD$  (bottom), respectively. The anticipated increase in the scattering intensity as the molecular weight of the PG increases is observed at low  $q$ .

Very similar behavior is observed in both solvents. Especially the behavior at low scattering vectors is interesting. The scattering intensity reached a plateau at low  $q$  in most cases, which demonstrates that entities with defined molar mass are present. This is not necessarily expected, since the high functionality of hydroxyl groups could lead to strong aggregation in

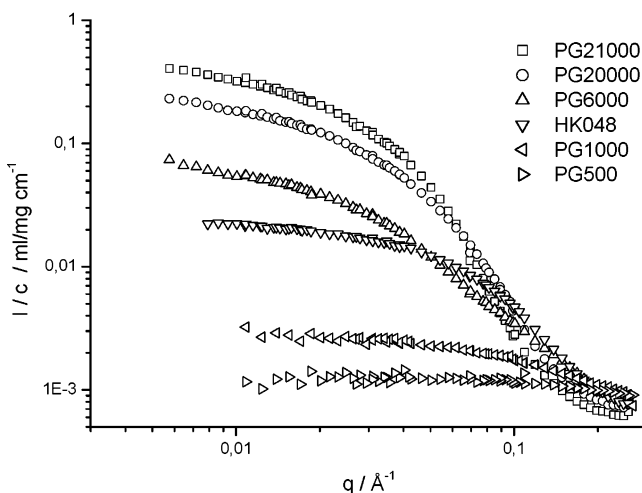
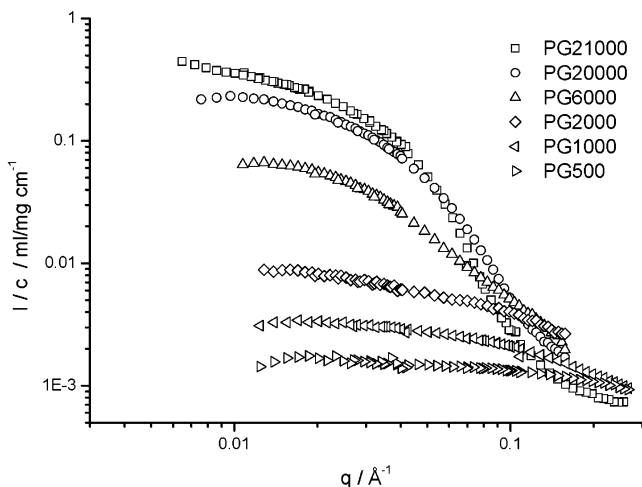


**Figure 1.** SANS data  $I(q)/c$  vs  $q$  for different samples of hyperbranched polyglycerols in  $D_2O$  (top) and  $CD_3OD$  (bottom).

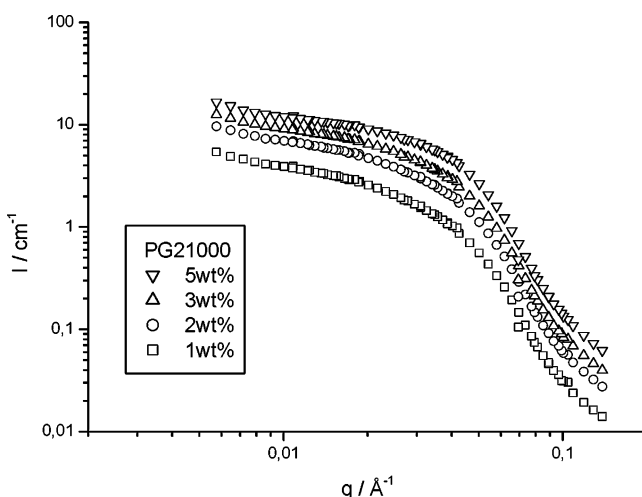


**Figure 2.** Scattering curves for sample PG21000 at different concentrations in  $D_2O$ .

aqueous solution as it is known e.g. from polysaccharides and other water-soluble polymers. Apparently, the hyperbranched structure prevents strong aggregation.

A concentration series in aqueous solution was investigated for two samples, and scattering curves of sample PG21000 between 1 and 5 wt % are shown in Figure 2. The shape of the curves is the same, but normalization with concentration did not lead to an

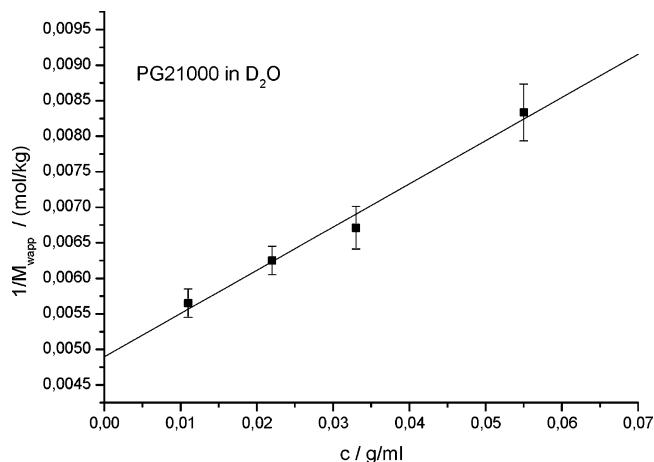


**Figure 3.** Concentration dependence of apparent molar mass for sample PG21000 in  $D_2O$ .

overlap. The influence of polymer interactions is obvious from Figure 3, where the concentration dependence of the reciprocal apparent molecular weight is displayed. A linear dependence is found, and the extrapolation according to eq 3 provides  $M_w = 204 \pm 8$  kg/mol and  $A_2 = (0.3 \pm 0.03) \times 10^{-4}$  mol  $cm^3$   $g^{-2}$ . (To determine  $M_w$ , the contrast factor needs to be calculated, and the scattering length density of the repeating unit depends on the composition of the monomer. In this study, we assumed full exchange of the hydroxyl protons vs D in both solvents.)

Table 1 summarizes the results for all samples. Since we could not study concentration series for all samples, the values obtained in dilute solution 1 wt % are listed. However, the difference between true and apparent molar mass will be small for the low molar mass samples. The table also contains  $R_g$  values obtained from different data analysis as is discussed below.

Additional information on the structure of the macromolecules is obtained from the angular dependence of the scattering intensity. Figure 4 shows Kratky plots for the two largest polymers in aqueous solution. The results are very similar to those obtained by de Luca et al. on hyperbranched polymers in organic solvents. The development of a peak in the Kratky plot is indicative of compact structures.

The results obtained in the two solvents agree very well. The differences in the calculated molar masses can be caused by errors in the calculated scattering contrast and the extrapolation to zero scattering angle. It is known e.g. for poly(ethylene oxide) that a hydration shell changes the scattering contrast. Thus, absolute determination of  $M_w$  is very difficult for these materials with SANS. However, this does not influence comparisons within a series of samples with different molar mass.

The observation that the values of  $M_{app}$  and  $R_g$  in the two solvents  $D_2O$  and  $CD_3OD$  agree so well indicates that stable solutions are obtained in both cases. We wish to note that it cannot unambiguously be excluded that the scattering objects are formed by a closed aggregation of smaller macromolecules. Also, because of the limited  $q$  range of neutron scattering, the formation of very large aggregates is difficult to detect. However, since a very similar behavior is found in the two solvents, it seems reasonable to assume that essentially singly dispersed hyperbranched macromolecules are present in dilute solution in both solvents.

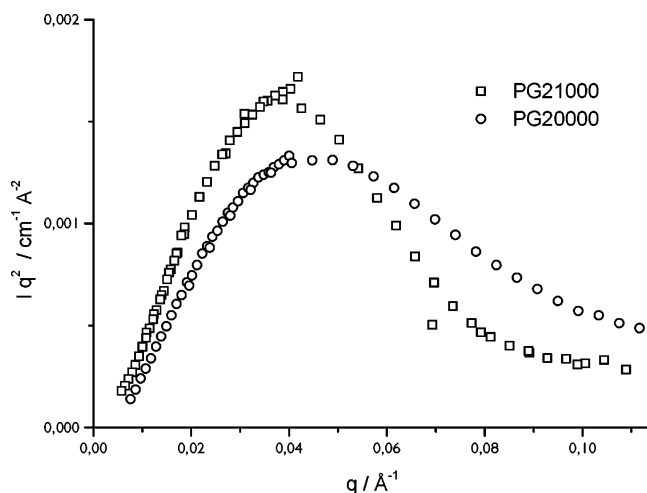
**Table 1. Apparent Molecular Weight and Radius of Gyration for Polyglycerols in D<sub>2</sub>O and CD<sub>3</sub>OD**

sample	<i>c</i> in D <sub>2</sub> O, g L <sup>-1</sup>	<i>M</i> <sub>app</sub> in D <sub>2</sub> O, kg mol <sup>-1</sup>	<i>R</i> <sub>g</sub> in D <sub>2</sub> O Guinier, nm	<i>R</i> <sub>g</sub> in D <sub>2</sub> O Kratky, nm	<i>c</i> in CD <sub>3</sub> OD, g L <sup>-1</sup>	<i>M</i> <sub>app</sub> in CD <sub>3</sub> OD, kg mol <sup>-1</sup>	<i>R</i> <sub>g</sub> in CD <sub>3</sub> OD Guinier, nm	<i>R</i> <sub>g</sub> in CD <sub>3</sub> OD Kratky, nm
PG21000	11	178	4.7	6.1	17.8	226	7	6.5
PG20000	11	150	5.6	5.6	17.8	122	6.2	5.6
PG6000	11	42	4.3		17.8	34.7	2.7	2.5
HK048					17.8	14	2.7	2.5
PG2000	11	3.8	1.3					
PG1000	22	1.9	1.5		22	1.3	1.3	
PG500	22	0.94	1		23	0.58		

Further structural information is obtained from the dependence of the radius of gyration on molar mass. Fractal objects are characterized by  $R_g \propto M^{1/d_f}$ , where  $d_f$  denotes the fractal dimension.  $d_f$  can be affected by polydispersity in the case of extremely broad molar mass distribution,<sup>24</sup> and then the slope in the double-logarithmic plot of  $R_g$  vs  $M$  yields an effective fractal dimension. Figure 5 displays such double-logarithmic plots of  $R_g$  vs  $M_{app}$  for 1 wt % solutions in D<sub>2</sub>O (top) and CD<sub>3</sub>OD (bottom), respectively. Although the error in  $R_g$  especially at low molar mass is rather large, a linear dependence is obvious in both plots. The slopes of the lines in Figure 5 are  $0.33 \pm 0.03$  for D<sub>2</sub>O and  $0.32 \pm 0.05$  for CD<sub>3</sub>OD solutions and thus are very close to  $1/3$ , which is found for spheres. Obviously, the hyperbranched macromolecules form very compact structures in both solvents. The slopes can be compared to the results by Gelade et al.<sup>11</sup> and de Luca et al.,<sup>12</sup> who found slopes of 0.6 and 0.4, respectively. In the latter cases organic solvents were studied. Apparently the polyglycerols are more compact.

A second approach for the determination of fractal dimensions employs the  $q$  dependence of the scattering intensity, which for fractal objects is given as  $P_{fractal}(q) \propto q^{-d_f}$ . The fractal concept holds only within an intermediate  $q$  range limited by the radius of gyration and segment length. To obtain reliable values for the fractal dimensions, the power law region needs to extend at least over 1 order of magnitude in  $q$ . In the above-mentioned investigations, Gelade et al. and de Luca et al. observed that the scattering curves of samples with different molecular weight overlapped in the high  $q$  region, and the fractal dimension could be obtained from the linear region.

The data in Figure 1 reveal that such an overlap was not found in the case of the polyglycerol solution, indicating that the internal structure is not perfectly identical for the different samples. The  $q$  dependence

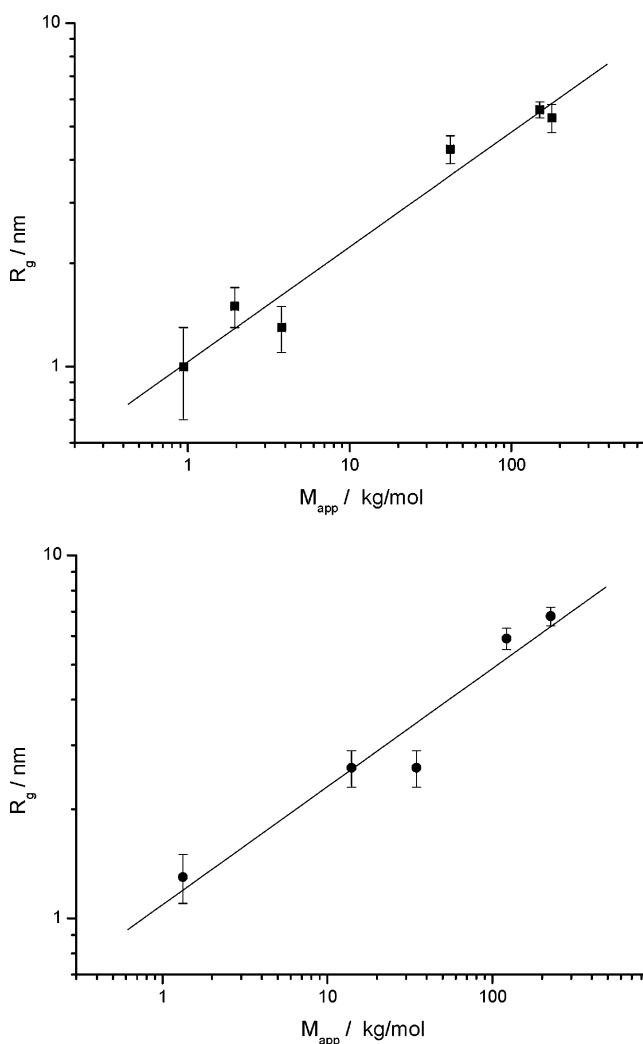
**Figure 4.** Kratky plots for two hyperbranched polyglycerols in D<sub>2</sub>O.

shows a power law region only over a limited  $q$  range, and consequently a fractal dimension was not determined. However, the data for the largest polymers reveal that the slope in the intermediate  $q$  region becomes slightly steeper, indicating that the polymers become more compact and develop a well-defined surface.

Further support for the compact spherelike structure is obtained from the second virial coefficient  $A_2$ . For hard spheres  $A_2$  is related to particle mass  $M$  and volume  $V_{hs}$  as<sup>25</sup>

$$A_2 = \frac{4N_L V_{hs}}{M^2} \quad (7)$$

and an equivalent thermodynamic hard-sphere radius

**Figure 5.** Double-logarithmic representation of radius of gyration vs apparent molar mass (determined at a concentration of 1 wt %) for hyperbranched polyglycerols in D<sub>2</sub>O (top) and CD<sub>3</sub>OD (bottom).

**Table 2. Results from SANS of Hyperbranched Poly(glycerol ester)s in C<sub>6</sub>D<sub>6</sub>**

sample	polyglycerol core	deg of derivatization, %	c, %	$M_{app}$ , kg mol <sup>-1</sup>	$R_g$ (Guinier), nm	$R_g$ (Kratky), nm
PG6000-C15 <sub>0.22</sub>	PG6000	22	1	325	79	12.2
PG6000-C15 <sub>0.22</sub>	PG6000	22	2	409	78	11.6
PG6000-C15 <sub>0.22</sub>	PG6000	22	3	433	80	11.7
PG6000-C15 <sub>0.22</sub>	PG6000	22	5	491	79	11.1
PG6000-C15 <sub>0.48</sub>	PG6000	48	1	41	5.4	4.5
PG6000-C15 <sub>0.77</sub>	PG6000	77	1	46	4.9	4.4
PG6000-C15 <sub>1.00</sub>	PG6000	100	1	52	4.6	4.9
PG6000-C15 <sub>1.00</sub>	PG6000	100	2	58.7	4.8	4.9
PG6000-C15 <sub>1.00</sub>	PG6000	100	3	54.6	4.8	5.1
PG6000-C15 <sub>1.00</sub>	PG6000	100	5	48.5	4.7	4.9
PG2000-C15 <sub>0.71</sub>	PG2000	71	1		1.4	2.6
PG20000-C15 <sub>0.76</sub>	PG20000	76	1		6.6	6.5
PG20000-C15 <sub>0.47</sub>	PG20000	47	1		6.6	6.3

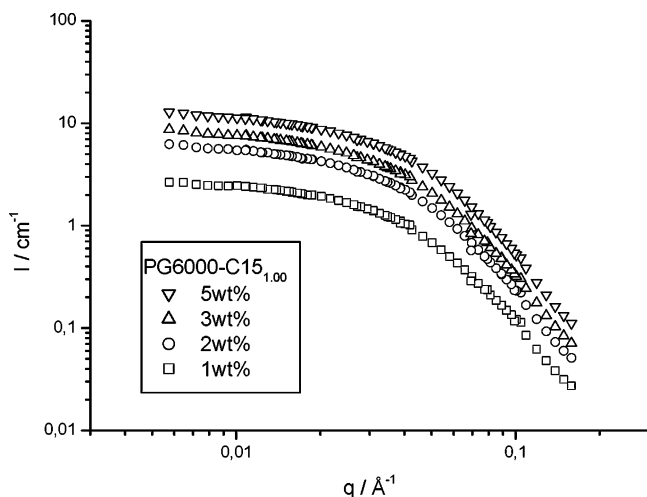
$\eta_{hs}$  can be calculated. With the above-mentioned values for sample PG21000 we obtained  $\eta_{hs} = 5$  nm, which agrees nicely with the size obtained from the angular dependence of the scattering intensity.

**Hyperbranched Poly(glycerol ester)s.** Amphiphilic poly(glycerol ester)s were synthesized based on the hyperbranched polyglycerols. These polymers are soluble in apolar organic solvents and can be used for various applications as e.g. the preparation of metal nanocolloids.<sup>15</sup>

Table 2 provides an overview of the samples investigated here and summarizes the SANS results. Poly(glycerol ester)s based on different polyglycerol cores and with different degree of esterification were studied.

Figure 6 displays scattering curves obtained by SANS from different concentrations of polymer PG6000-C15<sub>1.00</sub> in the solvent C<sub>6</sub>D<sub>6</sub>, where all hydroxyl groups have been derivatized. The scattering curves reveal a plateau at low  $q$ , and the curves nearly overlap when normalized by concentration. The second virial coefficient is small but slightly positive. Obviously, the polymer forms a stable solution, and no aggregation is found. In a Kratky plot of these data (not shown) the typical behavior of hyperbranched polymers is observed, and the radius of gyration obtained from the position of the maximum is concentration independent and agrees with that obtained from the Guinier analysis (see Table 2).

Different behavior was found with sample PG6000-C15<sub>0.22</sub> which has a lower degree of esterification of 22% (see Figure 7). The scattering curves did not reveal a plateau at low  $q$ , and the apparent molar mass increased with concentration, indicating that aggregates

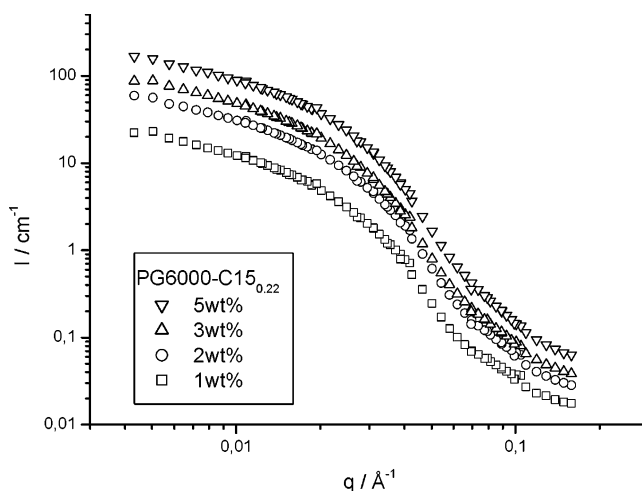
**Figure 6.** Scattering curves for poly(glycerol ester) PG6000-C15<sub>1.00</sub> at different concentrations in C<sub>6</sub>D<sub>6</sub>.

are formed in C<sub>6</sub>D<sub>6</sub> solution that become larger with increasing concentration. Apparently, the high hydroxyl group functionality is not sufficiently shielded by the long alkyl chains to prevent aggregation in this solvent.

We further investigated two samples at intermediate degree of esterification (48 and 77%, respectively) based on the same hyperbranched polyglycerol core at a dilute solution of 1 wt %. In both cases, a small apparent molecular weight and small radius of gyration were observed. This indicates that a degree of derivatization of ca. 50% leads to a stable solution of single amphiphilic hyperbranched polymers. A Kratky plot for the samples with different degrees of esterification is shown in Figure 8, and the different properties of sample PG6000-C15<sub>0.22</sub> can be clearly seen.

A comparison of the samples with 48, 77, and 100% degree of esterification shows that the molar mass increases whereas  $R_g$  stays nearly constant; thus, the structure becomes more compact when more alkyl chains are introduced. This indicates that during the esterification process the outer hydroxyl groups react first.

Table 2 also contains data from poly(glycerol ester)s based upon other polyglycerol cores. Samples PG20000-C15<sub>0.76</sub> and PG20000-C15<sub>0.47</sub> are derivatives of the bigger polyglycerol core PG20000, and consequently the radius of gyration of the esters in organic solution is bigger as compared to the polymers based on the PG6000 core. The degree of esterification does not influence the size, in agreement with what was found with samples PG6000-C15<sub>1.00</sub> and PG6000-C15<sub>0.48</sub> and again shows that the structure becomes more compact when more alkyl chains are present.

**Figure 7.** Scattering curves for poly(glycerol ester) sample PG6000-C15<sub>0.22</sub> at different concentrations in C<sub>6</sub>D<sub>6</sub>.

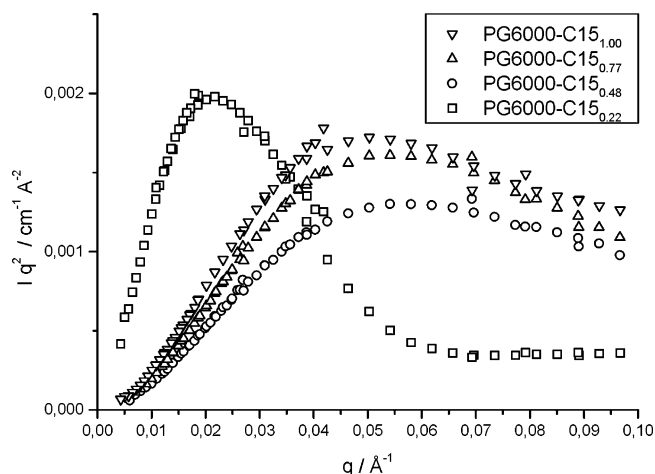


**Figure 8.** Kratky plots for poly(glycerol ester)s at different degree of esterification in  $C_6D_6$ .

Samples PG2000-C15<sub>0.71</sub>, PG6000-C15<sub>0.48</sub>, and PG2000-C15<sub>0.47</sub> all have an intermediate degree of derivatization, and  $R_g$  increases with increasing molar mass of the core. Obviously, the size of the poly(glycerol ester)s mainly depends on the size of the hyperbranched polyglycerol core when the number of alkyl chains is sufficient to obtain a stable solution without aggregation.

### Conclusions

The solution structure of hyperbranched macromolecules was investigated by means of SANS.

The most relevant result of the present study is the observation of similar particles sizes and molar masses of the hyperbranched polyglycerols in  $D_2O$  and  $CD_3OD$ , respectively. Obviously, small well-defined entities are present in both solvents, despite the high functionality of hydroxyl groups that could lead to strong aggregation. Apparently, the hyperbranched structure prevents strong irregular aggregation in those solvents.

Kratky plots of the scattering intensity reveal a compact structure of the hyperbranched polyglycerols, which is also obvious from the scaling relation of the radius of gyration with molar mass from which a dimension of three was obtained.

Amphiphilic derivatives of the hyperbranched polyglycerols have been studied in the nonpolar solvent  $C_6D_6$ . Again, molecularly dispersed polymers are found provided the degree of esterification was sufficiently high. A low degree of derivatization of only 22% was not sufficient to prevent aggregation in  $C_6D_6$ . The macromolecules become more compact when the degree of esterification increases.

**Acknowledgment.** This work was supported by the VolkswagenStiftung (Schwerpunkt Komplexe Materi-

alien). H.F., H.K., and S.M. gratefully acknowledge financial support and fellowships from the Fonds der Chemischen Industrie FCI. U.S. is grateful for a Baden-Württemberg Landesgraduiersten stipend. S.M. thanks the Eugen Graetz-Foundation for financial support.

### References and Notes

- (1) Geddes, R. In *The Polysaccharides*; Aspinall, G. O., Ed.; Academic Press: London, 1985; Vol. 3, p 209 and references therein.
- (2) Flory, P. J. *Principles of Polymer Chemistry*; Cornell University Press: Ithaca, NY, 1952.
- (3) Frey, H.; Haag, R. *Mol. Biotechnol.* **2002**, *90*, 257.
- (4) Bosman, A.; Janssen, H. M.; Meijer, E. W. *Chem. Rev.* **1999**, *99*, 1655.
- (5) Hawker, C. J. *Curr. Opin. Colloid Interface Sci.* **1999**, *4*, 117.
- (6) Newkome, G. R.; He, E.; Moorefield, C. N. *Chem. Rev.* **1999**, *99*, 1689.
- (7) Frechet, J. M. J.; Hawker, C. J.; Gitsov, I.; Leon, J. W. *Pure Appl. Chem.* **1996**, *A33*, 1399.
- (8) Radke, W.; Litvinenko, G.; Müller, A. H. E. *Macromolecules* **1998**, *31*, 239.
- (9) Hanselmann, R.; Hölter, D.; Frey, H. *Macromolecules* **1998**, *31*, 3790.
- (10) Sunder, A.; Hanselmann, R.; Frey, H.; Muelhaupt, R. *Macromolecules* **1999**, *32*, 4240.
- (11) Gelade, E. T. F.; Goderis, B.; de Koster, C. G.; Meijerink, N.; van Benthem, R. A. T. M.; Fokkens, R.; Nibbering, N.; Mortensen, K. *Macromolecules* **2001**, *34*, 3552.
- (12) de Luca, E.; Richards, R. W.; Grillo, I.; King, S. M. *J. Polym. Sci., Part B: Polym. Phys.* **2003**, *41*, 1352.
- (13) Sunder, A.; Krämer, M.; Hanselmann, R.; Mülhaupt, R.; Frey, H. *Angew. Chem.* **1999**, *111*, 3758.
- (14) Stiriba, S.-E.; Kautz, H.; Frey, H. *J. Am. Chem. Soc.* **2002**, *124*, 9698.
- (15) (a) Mecking, S.; Thomann, R.; Frey, H.; Sunder, A. *Macromolecules* **2000**, *33*, 3958. (b) Schlotterbeck, U.; Aymonier, C.; Thomann, R.; Hofmeister, H.; Tromp, M.; Richtering, W.; Mecking, S. *Adv. Funct. Mat.*, in press.
- (16) Mecking, S.; Schlotterbeck, U.; Thomann, R.; Soddemann, M.; Stieger, M.; Richtering, W.; Kautz, H. *Polym. Mater. Sci. Eng.* **2001**, *84*, 511.
- (17) Aymonier, C.; Schlotterbeck, U.; Antonietti, L.; Zacharias, P.; Thomann, R.; Tiller, J. C.; Mecking, S. *Chem. Commun.* **2002**, 3018.
- (18) Sablong, R.; Schlotterbeck, U.; Vogt, D.; Mecking, S. *Adv. Synth. Catal.* **2003**, *345*, 333.
- (19) Slagt, M. Q.; Stiriba, S.-E.; Klein Gebbink, R. J. M.; Kautz, H.; Frey, H.; van Koten, G. *Macromolecules* **2002**, *35*, 5734.
- (20) Stiriba, S.-E.; Slagt, M. Q.; Kautz, H.; Klein Gebbink, R. J. M.; Thomann, R.; Frey, H.; van Koten, G. *Chem.-Eur. J.*, in press.
- (21) Stuhmann, H. B.; Burkhard, N.; Dietrich, G.; Junemann, R.; Meerwin, W.; Schmitt, M.; Wadzack, J.; Willumeit, R.; Zhao, J.; Nierhaus, K. H. *Nucl. Instrum. A* **1995**, *356*, 124.
- (22) Schurtenberger, P. In *Neutrons, X-rays and Light Scattering Methods Applied to Soft Condensed Matter*; North-Holland Delta Series; Lindner, P., Zemb, Th., Eds.; Elsevier: Amsterdam, 2002; pp 147–170.
- (23) Burchard, W. *Macromolecules* **1977**, *10*, 919.
- (24) Daoud, M.; Family, F.; Jannink, J. *J. Phys., Lett.* **1984**, *45*, L199.
- (25) McQuarrie, D. A. *Statistical Mechanics*; Harper & Row: New York, 1973.